Phosphotyrosine-dependent activation of Rac-1 GDP/GTP exchange by the *vav* proto-oncogene product

Piero Crespo*†, Kornel E. Schuebel‡, Amy A. Ostrom‡, J. Silvio Gutkind* & Xosé R. Bustelo‡

* Molecular Signaling Unit, Laboratory of Cellular Development and Oncology, National Institute of Dental Research, National Institutes of Health, Bethesda, Maryland 20892, USA
† Departamento de Biologia Molecular, Facultad de Medicina, Universidad de Cantabria, Santander 39011, Cantabria, Spain
‡ Department of Pathology, School of Medicine and University Hospital, State University of New York at Stony Brook, Stony Brook, New York 11794, USA

THE oncogenic protein Vav[1,2] harbours a complex array of structural motifs, including leucine-rich, Dbl-homology, pleckstrin-homology, zinc-finger, SH2 and SH3 domains. Upon stimulation by antigens or mitogens, Vav becomes phosphorylated on key tyrosine residues[3–5] and associates with other signalling proteins, including the mitogen receptors[3,4] Zap-70 (ref. 6), Vap-1 (ref. 5) and Slp-76 (ref. 7). Disruption of the *vav* locus by homologous recombination causes severe defects in signalling by primary antigen receptors, leading to abnormal lymphocyte proliferation and lymphopenia[8,9]. Despite the importance of Vav cell signalling, the function of this protein remains unknown. Here we show that tyrosine-phosphorylated Vav, but not the non-phosphorylated protein, catalyses GDP/GTP exchange on Rac-1, a protein implicated in cell proliferation and cytoskeletal organization[10,11], causing this GTPase to switch from its inactive to its active state. Transfection experiments also show that phosphorylation of Vav on tyrosine residues leads to nucleotide exchange on Rac-1 *in vivo* and stimulates c-Jun kinase, a downstream element in the signalling pathway involving this GTPase. Our results have identified a function for Vav and define a mechanism in which engaged membrane receptors activate its signalling pathway.

We have previously shown that Vav is located upstream of Rac-1 (ref. 12). Because Vav contains a DH (Dbl-homology) domain usually present in guanine-nucleotide-exchange factors (GEFs) that act for GTPases of the Rho/Rac family[11], we investigated whether Vav had similar enzyme activity towards Rac-1. Initial efforts using either full-length, oncogenic Vav protein or isolated domains were unsuccessful (data not shown). As Vav becomes extensively phosphorylated on tyrosine residues upon activation of protein tyrosine kinases[3–5], we investigated whether this post-translational modification could influence Vav GDP/GTP-exchange activity. A hexahistidine-tagged Vav protein was incubated with ATP in the presence or absence of a glutathione *S*-transferase (GST) protein containing the protein tyrosine kinase Lck, a member of the Src family[13]; the GDP/GTP exchange activity of Vav was then assessed by following the incorporation of [^{35}S]GTP-γS into GDP-loaded Rac-1 in a filter immobilization assay. Figure 1*a* shows that preincubation of Vav with GST–Lck fusion protein stimulated the exchange activity of Vav towards Rac-1 protein. Non-phosphorylated Vav caused little GDP/GTP exchange even after 45 min at room temperature, with results being the same as those for Rac-1 and the GST–Lck fusion protein alone (Fig. 1*a*, left). The kinetics of Rac-1 GDP/GTP exchange induced by phosphorylated Vav were similar to those obtained with Cdc42 and its bonafide GEF, the *dbl* oncogene product[11], under the same conditions (Fig. 1*a*, right). However, unlike Vav, incubation with GST–Lck did not affect the catalytic activity of Dbl (Fig. 1*a*, right), so upregulation of Vav by this protein tyrosine kinase is not a general feature of all DH family members. We also analysed the effect of Vav on the incorporation

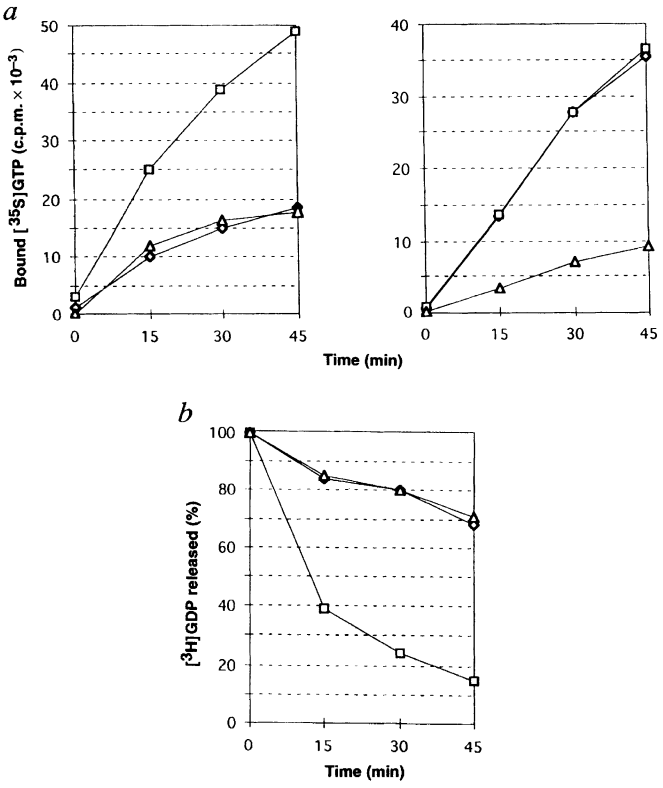

FIG. 1 *a*, Incorporation of [^{35}S]GTP-γS in Rac-1 mediated by Vav protein. Left, GDP-loaded Rac-1 was incubated with 5 μM [^{35}S]GTP-γS in the presence of phosphorylated Vav (squares), non-phosphorylated Vav (diamonds), or autophosphorylated GST–Lck (triangles). At each time point, aliquots were taken in duplicate and the GTP bound to Rac-1 was evaluated in a filter-immobilization assay. Right, GDP-loaded Cdc42 was subjected to exchange reactions in the presence of either Dbl plus GST–Lck (squares), Dbl alone (diamonds), or autophosphorylated GST-Lck (triangles). *b*, Kinetics of Rac-1 [^{3}H]GDP release in the presence of 1 mM GTP and the combination of proteins indicated in *a* (left).

of cold GTP into [^{3}H]GDP-loaded Rac-1 (Fig. 1*b*) and found that when it is tyrosine-phosphorylated, Vav enhances the dissociation of [^{3}H]GDP from Rac-1 compared with either non-phosphorylated Vav or autophosphorylated GST–Lck protein.

We investigated the specificity of this enzyme by GDP/GTP exchange assay on Ras-family substrates. Phosphorylated Vav was less effective at stimulating nucleotide exchange on RhoA protein than on Rac-1 under the same conditions (Fig. 2*a*). There was no significant effect when Cdc42, Ran or H-Ras were included in the incubations (Fig. 2*a*). The lack of Vav exchange activity on H-Ras is in agreement with earlier results indicating that *vav* transformation is independent of Ras function[14]. We conclude that Vav is acting *in vitro* as a Rac-1 GEF and that this activity is modulated by tyrosine phosphorylation.

The Vav protein is oncogenically activated as a result of an amino-terminal deletion (residues 1–66). This truncated protein is 20-fold more active than the wild type, as determined by focus formation assay in rodent fibroblasts[2]. To determine whether truncation results in constitutively active Vav, we compared its exchange activity with full-length Vav and found that both proteins were dependent on phosphorylation for their activation (Fig. 2*b*). This suggests that tyrosine phosphorylation *per se* cannot account for the different activity of the proto- and oncogenic Vav proteins *in vivo*. Activation of Vav *in vivo* might also depend on the elimination of an inhibitory component constitutively associated with its N terminus, the nature of which is under investigation.

To confirm the role of Vav as a Rac-1 GEF, we tested whether expression of the Vav oncoprotein could promote guanosine-

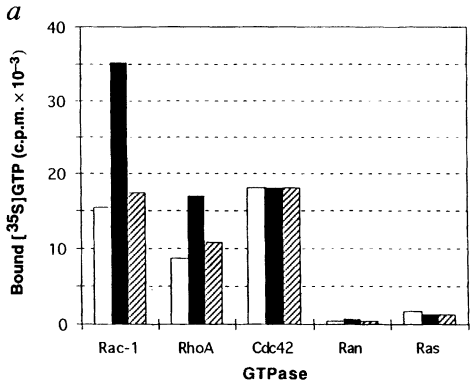

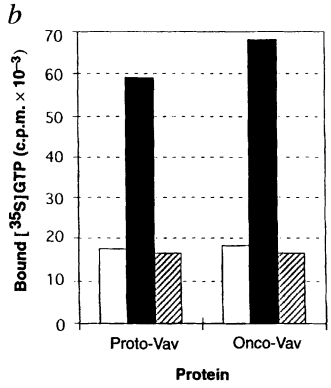

nucleotide exchange on Rac-1 in living cells. Because Rho/Rac proteins have high intrinsic GTPase activity which precludes detection of their GTP-bound forms *in vivo*[15], we used ^{32}P-labelled GDP bound to these proteins to evaluate their nucleotide-exchange rates[16]. AU5-epitope-tagged Rac-1, RhoA, Cdc42 or H-Ras were expressed in COS-7 cells either alone or in combination with oncogenic Vav; cells were transfected, starved, incubated briefly with [^{32}P]orthophosphate, and nucleotide exchange was determined by counting the GDP in anti-AU5 immunoprecipitates after thin-layer chromatography[16]. Co-transfection of the *vav* oncogene with AU5–Rac-1 caused a sevenfold increase in ^{32}P-labelled GDP bound to Rac-1, but there was no exchange upon co-transfection with AU5–H-Ras or AU5–RhoA; a small exchange was detected for AU5–Cdc42 (Fig. 3*a*, top). As before[16], incorporation of labelled GDP on these GTPases was low when transfected on their own so they probably undergo minimal nucleotide exchange in quiescent conditions (Fig. 3*a*). Western blotting confirmed that all proteins were expressed in each transfection (Fig. 3*a*, bottom panel). As an additional control, nucleotide exchange was routinely activated on RhoA and Cdc42 upon co-transfection with Dbl, and on H-Ras with SOS or Ras GRF/Cdc25^{Mm} (ref. 11) (data not shown), demonstrating that these GTPases are active in our system.

Coexpression of the *vav* oncogene with Rac-1 N17, a dominant-negative mutant that is blocked in the inactive, GDP-loaded form, gave no incorporation of ^{32}P-labelled nucleotide in Rac-1, con-

◀ FIG. 2 *a*, Specificity of Vav enzyme activity. Autophosphorylated GST–Lck (hatched boxes), phosphorylated Vav (black boxes), and non-phosphorylated Vav (white boxes) were subjected to exchange reactions in the presence of the indicated GDP-loaded GTPases for 45 min (see Methods). *b*, Phosphorylation-dependent exchange activity of wild-type and oncogenic Vav proteins. GDP-loaded Rac-1 was incubated with [^{35}S]GTP-γS in the presence of GST–Lck (hatched boxes), phosphorylated (black boxes) or non-phosphorylated (white boxes) Vav proteins. After 45 min, duplicate aliquots were used to determine ^{35}S-labelled GTP incorporated in Rac-1 (see Methods).

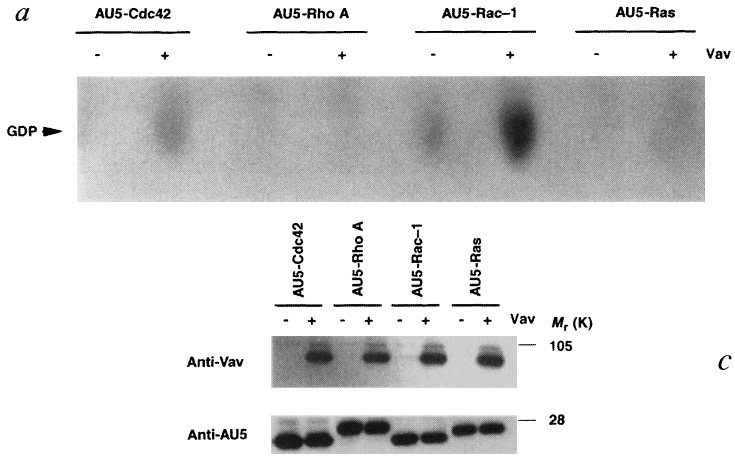

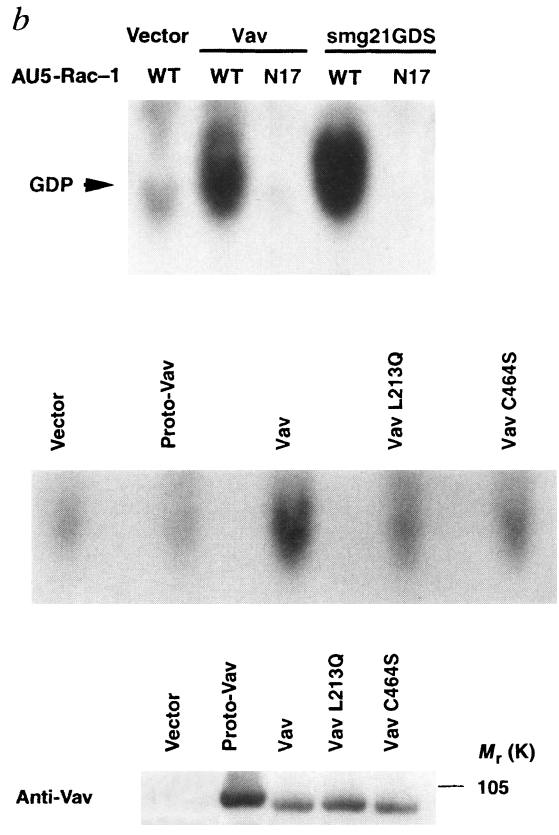

FIG. 3 *a*, Effect of the *vav* oncogene product on Ras-family nucleotide exchange *in vivo*. Top, nucleotide loading of GTPases in the absence (−) or presence (+) of the *vav* oncogene product. Bottom, expression of Vav and GTPases in COS-7 cells, as determined by anti-Vav[5] and anti-AU5 (Babco) immunoblot analysis. *b*, Effect of Vav oncoprotein and smg21GDS on the nucleotide loading of wild type (WT) and a dominant-negative mutant (N17) version of Rac-1. *c*, Activation of Rac-1 by Vav proteins *in vivo*. Top, nucleotide loading on Rac-1 in the presence of the *vav* proto-oncogene (Proto-Vav), the *vav* oncogene (Vav), and two inactive mutant versions of the *vav* oncogene. Bottom, expression of Vav proteins in COS-7 cells, as determined by anti-Vav immunoblot analysis.

firming that the effect observed in the Vav/Rac-1 co-transfection did reflect an increase in guanine-nucleotide-exchange rate (Fig. 3*b*). This effect is identical to that of the smg21 guanine-nucleotide-dissociation factor[11] (Fig. 3*b*). Anti-AU5 immunoblot analysis of cell lysates from parallel transfections showed that both forms of Rac-1 were comparably expressed (data not shown). In addition, co-transfection of wild-type Rac-1 with either the *vav* proto-oncogene product or two inactive versions of the Vav oncoprotein with point mutations in the DH motif (L213Q) (ref. 12) or in the cysteine-rich region (C464S) (refs 2, 12) resulted in much slower nucleotide exchange on Rac-1 *in vivo* (Fig. 3*c*). This agrees with the low activity of these proteins in both focus-formation[2] and c-Jun kinase (JNK) activation experiments[12] and supports the idea of a linear pathway between Vav, Rac-1 and JNK proteins.

To test whether the activity of the *vav* proto-oncogene product was enhanced by tyrosine phosphorylation, we determined the nucleotide-exchange rate of Rac-1 *in vivo* after co-transfection of the *vav* proto-oncogene with plasmids encoding wild-type or constitutively active mutants of two Src-family members, Lck and Fyn (ref. 13). Although expression of each of these signalling proteins alone did not cause Rac-1 nucleotide exchange, coexpression of the *vav* proto-oncogene with either form of Lck or Fyn synergistically increased ^{32}P-nucleotide incorporation on Rac-1 (Fig. 4*a*).

We next examined whether coexpresison of the *vav* proto-oncogene product (proto-Vav) with Lck and Fyn allowed stimulation of JNK, a downstream element of the Vav pathway that is activated in a Rac-1-dependent manner[12]. A haemagglutinin (HA)-tagged version of JNK was transfected in COS-7 cells either alone or in combination with proto-Vav and wild-type and constitutively active mutants of Lck and Fyn. Expression of Lck and Fyn alone failed to activate JNK, and expression of proto-Vav alone only weakly stimulated JNK (Fig. 4*b*); in contrast, coexpression of proto-Vav with either Lck or Fyn proteins increased JNK activity (3- to 4-fold), reaching ~60% of levels obtained upon expression of the *vav* oncogene (Fig. 4*b*). Both nucleotide exchange on Rac-1 and JNK activation upon co-transfection with Lck and Fyn correlated with the induction of tyrosine phosphorylation on proto-Vav under those transfection conditions, as determined by anti-phosphotyrosine immunoblot analysis of Vav immunocomplexes (Fig. 4*c*).

Our observations provide evidence for a role for Vav in Rac-1 activation and a mechanisms for stimulating this function during signal transduction by mitogenic and antigenic receptors. According to this model, extracellular stimulation results in phosphorylation of Vav on tyrosine residues and activation of its exchange activity towards Rac-1 and of its downstream elements, including the SEK/JNK serine/threonine cascade. To our knowledge, this is the first example of regulation of a small G protein by direct tyrosine phosphorylation of its GEF. Rac-1 and Vav have been implicated in several overlapping cellular functions, including mitogenesis[1,2,17,18], cooperativity with Ras[14,17,18], and regulation of NF-AT-dependent responses in T-cell lines[19,20]. We have shown previously that Rac-1 dominant-negative mutants, but not those of RhoA, Cdc42 or H-Ras, downregulate Vav signalling[12]. Considered with our latest results, this indicates that Rac-1 is an important effector molecule in the signalling cascade of the *vav* proto-oncogene product. □

Methods

Protein purification. Wild-type Vav was purified from Sf9 cells by using nickel columns (Qiagen) according to the manufacturer's recommendation. Vav oncoprotein was purified from Sf9 cell lysates using protein-A Sepharose beads coated with a polyclonal anti-Vav antibody raised against residues 576–589 of mouse Vav protein[2], followed by elution with saturating amounts of immunizing peptide. GST–Lck was purified from Sf9 as described[21]. A polyglutamic-tagged version of the *dbl* oncogene product purified from Sf9 cells was a gift from R. A. Cerione. GTPases were purified as GST fusion proteins according to standard procedures.

Expression vectors. Mammalian expression vectors encoding Vav (pcDNA derivatives) and GTPases (pCEV derivatives) have been described[12,22]. Constitutively active mutants of Src family proteins, including a truncated version of wild-type Fyn lacking the C-terminal 15 amino acids (FynC), as well as the Lck Y505F mutant (LckC), were expressed using pcDNA-derived vectors (Invitrogen).

Kinase and exchange reactions. Kinase reactions were done for 20–30 min at room temperature in 20 mM Tris–HCl, pH 7.5, 5 mM $MgCl_2$, 1 mM ATP. [^{35}S]GTP-γS was incorporated at room temperature[23] using 15 pmol GTPase, 4.5 pmol of either Vav or Dbl, and 3.5 pmol GST–Lck. [^{3}H]GDP release experi-

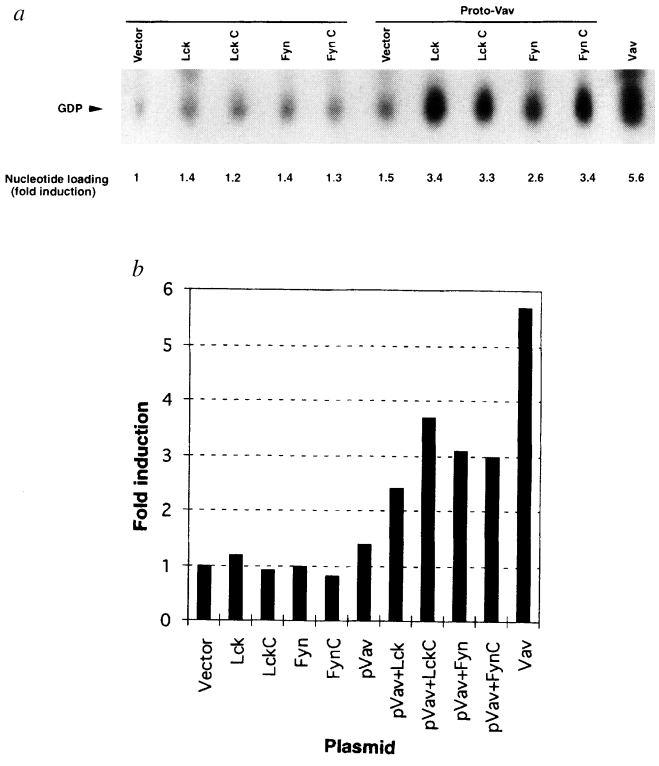

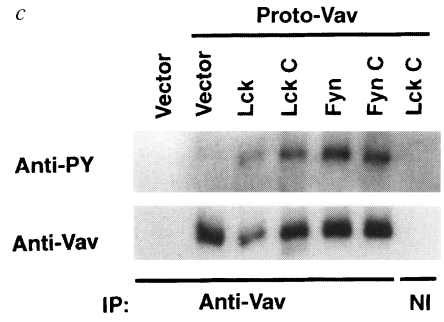

FIG. 4 *a*, Stimulation of Rac-1 nucleotide exchange rate *in vivo* by tyrosine phosphorylation of the *vav* proto-oncogene product. AU5-tagged Rac-1 was transfected in COS-7 cells either in the absence (–) or presence (Proto-Vav) of the *vav* proto-oncogene and wild-type Lck, Fyn and constitutively active (C suffix) mutants of the indicated Src family members. For comparative purposes, AU5-tagged Rac-1 was coexpressed with Vav. After transfection, relative guanosine-nucleotide-exchange rates on Rac-1 were determined as described in Methods. Values represent the mean of three independent experiments. *b*, Effect of tyrosine phosphorylation of wild-type Vav (pVav) on JNK activity. Cells were transfected and JNK activity determined using an immunocomplex kinase assay. Values represent the mean of three independent experiments. *c*, Levels of tyrosine phosphorylation of wild-type Vav in the presence of Src-family kinases. Lysates derived from COS-7 expressing the indicated signalling molecules were immunoprecipitated (IP) with either non-immune serum (NI) or a specific anti-Vav antibody. Final immunocomplexes were analysed on anti-phosphotyrosine (PY) or anti-Vav immunoblot.

ments were done as described[24] using 34 pmol GTPase, 3.4 pmol of either Vav or Dbl, and, when appropriate, 3.5 pmol GST–Lck.

JNK assay and *in vivo* nucleotide labelling of GTPases. COS-7 cells were transfected using DEAE–dextran[12]. After transfection, cells were cultured for 48 h, serum-starved in phosphate-free DMEM medium for 18 h, labelled with [^{32}P]orthophosphate (100 μCi ml^{-1}) for 2 h, and disrupted in lysis buffer (50 mM Tris-HCl, pH 7.5, 20 mM $MgCl_2$, 150 mM NaCl, 0.5% Nonidet-P40, 1 mM sodium orthovanadate, 1 mM PMSF, 25 μg ml^{-1} leupeptin and 25 μg ml^{-1} aprotinin). Lysates were immunoprecipitated with an anti-AU5 monoclonal antibody (Babco) for 1 h and immunocomplexes recovered using Gamma-bind G-Sepharose beads (Pharmacia/LKB). Immunoprecipitates were washed three times in lysis buffer, twice in 50 mM Tris-HCl, pH 7.5, 20 mM $MgCl_2$, 500 mM NaCl, and finally resuspended in 1 M KH_2PO_4, 5 mM EDTA, pH 8.0. Bound nucleotides were released by heating, and fractionated using polyethyleneimine thin-layer chromatography plates[16]. JNK activity was determined using an *in vitro* immunocomplex assay[12,22].

Received 24 September; accepted 18 November 1996.

1. Katzav, S., Martin-Zanca, D. & Barbacid, M. *EMBO J.* **8,** 2283–2290 (1989).
2. Coppola, J., Bryant, S., Koda, T., Conway, D. & Barbacid, M. *Cell Growth Differ.* **2,** 95–105 (1991).
3. Bustelo, X. R., Ledbetter, J. F. & Barbacid, M. *Nature* **356,** 68–71 (1992).
4. Margolis, B. *et al. Nature* **356,** 71–74 (1992).
5. Bustelo, X. R. & Barbacid, M. *Science* **256,** 1196–1199 (1992).
6. Katzav, S., Sutherland, M., Packham, G., Yi, T. & Weiss, A. *J. Biol. Chem.* **269,** 32579–32585 (1994).
7. Wu, J., Motto, D. G., Koretzky, G. A. & Weiss, A. *Immunity* **4,** 593–602 (1996).
8. Zhang, R., Alt, F. W., Davidson, L., Orkin, S. H. & Swat, W. *Nature* **374,** 470–473 (1995).
9. Tarakhovski, A. *et al. Nature* **374,** 467–470 (1995).
10. Ridley, A. J. *Curr. Opin. Genet. Dev.* **5,** 24–30 (1995).
11. Boguski, M. S. & McCormick, F. *Nature* **366,** 643–654 (1993).
12. Crespo, P. *et al. Oncogene* **13,** 455–460 (1996).
13. Bolen, J. B. *Cell Growth Differ.* **2,** 409–414 (1991).
14. Bustelo, X. R., Suen, K. L., Leftheris, K., Meyers, C. A. & Barbacid, M. *Oncogene* **9,** 2405–2413 (1994).
15. Zheng, Y., Hart, M. J. & Cerione, R. A. *Methods Enzymol.* **256,** 77–84 (1995).
16. Laudanna, C., Campbell, J. J. & Butcher, E. C. *Science* **271,** 981–983 (1996).
17. Qiu, R. G., Chen, J., Kirn, D., McCormick, F. & Symons, M. *Nature* **374,** 457–459 (1995).
18. Qiu, R. G., Chen, J., McCormick, F. & Symons, M. *Proc. Natl Acad. Sci. USA* **92,** 11781–11785 (1995).
19. Wu, J., Katzav, S. & Weiss, A. *Mol. Cell. Biol.* **15,** 4337–4346 (1995).
20. Genot, E., Cleverley, S., Henning, S. & Cantrell, D. *EMBO J.* **15,** 3923–3933 (1996).
21. Spana, C., O'Rourke, E. C., Bolen, J. B. & Fargnoli, J. *Protein Expr. Purif.* **4,** 390–397 (1993).
22. Coso, O. A. *et al. Cell* **81,** 1137–1146 (1995).
23. Horii, Y., Beeler, J. F., Sakaguchi, K., Tachibana, M. & Miki, T. *EMBO J.* **13,** 4776–4786 (1994).
24. Shou, C., Farnsworth, C. L., Neel, B. G. & Feig, L. A. *Nature* **358,** 351–354 (1992).

ACKNOWLEDGEMENTS. We thank the Bristol-Myers Squibb Pharmaceutical Research Institute, and M. Barbacid in particular, for providing most of the reagents used in this study. We also thank J. Glaven and R. A. Cerione for purified Dbl, Y. Takai for smg21 GDS cDNA, and N. Reich and M. Dosil for their help and support.

CORRESPONDENCE and requests for materials should be addressed to X.R.B. (e-mail: xbustelo@path.som.sunysb.edu).

Unusual Rel-like architecture in the DNA-binding domain of the transcription factor NFATc

Scot A. Wolfe*, Pei Zhou*, Volker Dötsch†, Lin Chen*, Angie You*, Steffan N. Ho‡, Gerald R. Crabtree‡, Gerhard Wagner† & Gregory L. Verdine*

* Department of Chemistry and Chemical Biology, Harvard University, Cambridge, Massachusetts 02138, USA
† Department of Biological Chemistry and Molecular Pharmacology, Harvard Medical School, Boston, Massachusetts 02115, USA
‡ Departments of Developmental Biology and Pathology, Howard Hughes Medical Institute, Stanford University Medical School, Stanford, California 94305, USA

TRANSCRIPTION factors of the NFAT family regulate the production of effector proteins that coordinate the immune response[1]. The immunosuppressive drugs FK506 and cyclosporin A (CsA) act by blocking a Ca^{2+}-mediated signalling pathway leading to NFAT. Although FK506 and CsA have enabled human organs to be transplanted routinely, the toxic side-effects of these drugs limit their usage. This toxicity might be absent in antagonists that target NFAT directly. As a first step in the structure-based search for NFAT antagonists, we now report the identification and solution structure of a 20K domain of NFATc (NFATc-DBD) that is both necessary and sufficient to bind DNA and activate transcription cooperatively. Although the overall fold of the NFATc DNA-binding domain is related to that of NF-κB p50 (refs 2, 3), the two proteins use significantly different strategies for DNA recognition. On the basis of these results, we present a model for the cooperative complex formed between NFAT and the mitogenic transcription factor AP-1 on the interleukin-2 enhancer.

NFAT consists of two clearly separable functional domains. The N-terminal domain of NFATc, residues 1 to 415, controls its subcellular localization in response to Ca^{2+}-mobilization (C. R. Beals and G.R.C., manuscript submitted). Residues 416 to 591 of NFATc (NFATc-DBD), are necessary and sufficient for DNA binding and transcriptional activation on the distal antigen-receptor response element of the interleukin (IL)-2 enhancer (ARRE2)[4] (S.N.H. and G.R.C., unpublished results). *In vitro*, NFATc-DBD cooperates with AP-1 to form a tight, oriented complex on ARRE2 (ref. 5). Furthermore, NFATc-DBD alone binds specifically to ARRE2, albeit more weakly than full-length NFATc. NFATc-DBD thus represents the core functional domain of human NFATc, similar to that identified for murine NFATp (ref. 6).

The core structural motif of NFATc-DBD consists of a ten-stranded antiparallel β-barrel (Fig. 1*a*, *b*) assembled by the packing of three β-sheets. The two primary sheets (βIHCFE and βABG) form the core of the β-barrel, with the third sheet (βDG′) capping off one end. Devoid of α-helical structure, the remainder of NFATc-DBD is composed of loops, two of which are especially prominent (βA–βB and βG′–βH loops). As commonly observed for surface projections in NMR structures, the conformations of the two prominent loops in NFAT-DBD vary widely among the family of calculated structures shown in Fig. 1*a*. The origin of this behaviour, revealed through ^{15}N-relaxation measurements[7] (data not shown), was found to differ for the two loops. Whereas the βG′–βH loop has high conformational mobility throughout, the majority of the βA–βB loop is conformationally constrained, except at residues 28–35 near the tip (Fig. 1*c*), which appear to be only partially ordered.

NFAT family members share extensive sequence homology (~70%) over a ~300-amino-acid region comprising the entire DNA-binding domain, the N-terminal half of which corresponds to NFATc-DBD[8]. A potential sequence relationship between the DNA-binding domain of NFAT and members of the NF-κB/Rel protein family has been noted[9,10]; however, the extent of sequence similarity (<20%) falls below that considered to be statistically significant. Comparison of the solution structure of NFATc-DBD with the X-ray structure of NF-κB p50 DNA-binding domain (Fig. 2) reveals that the two share an essentially identical overall fold (Fig. 2*a*, *b*) and strand topology (Fig. 2*c*, *d*). Many of the residues that are invariant between NFAT family members and p50 (Fig. 1*c*, bold) form the hydrophobic core of the β-barrel; the packing interface between the βAB and βHI strands is nearly identical in the two classes of proteins. The sequence is also highly conserved throughout much of the βG′ and βH strands, because both faces of the small βG′H sheet are important: side chains on one face project inwards to establish the protein core, whereas those from the other face (Ile 123, Val 147) make stabilizing contacts to the lower end of the βA–βB loop (Val 38). Several other invariant residues, especially prolines 21, 46, 58, 110 and 156 in NFAT, are